Self-Similar Structures Near the Edges of Strained Elastic Sheets

Michael Simkin
Advisor: Prof. Raz Kupferman

1 Abstract

Casual observation shows that interesting shapes arise when thin elastic sheets are deformed. For instance, a torn plastic bag has wrinkles along the torn edge. Closer inspection reveals that these shapes follow well-defined patterns - they are often self-similar. This was first reported in [1]. The question arises as to why self-similar structures are preferred in these cases. The explanation proposed in [1] attempts to explain this through minimization of the elastic energy of the system. In this approach, when deformed, the thin elastic material is endowed with a non-Euclidean 2-dimensional metric. Then, both deviation from the endowed metric and bending of the material are penalized by an increase in elastic energy (stretching and bending energy, respectively), and the material assumes the shape that minimizes this energy. As will be explained, in very thin sheets the metric deviation is the dominant contributor, so shapes closer to isometric embeddings are preferred. It is thought that this is the key to understanding the self-similarity, as perhaps there is a connection between isometric embeddings and self-similarity.

In a 2002 article ([2]), Basile Audoly and Arezki Boudaoud (henceforth A&B) investigated the energy minimization and self-similarity numerically. The main objective of my project was to follow the same path, in order to achieve a better understanding of A&B's results.

2 Notation

There are several notational shorthands used throughout this report.

Let

$$f(u,v) : \Omega \subseteq \mathbb{R}^2 \to \mathbb{R}$$

Then:

$f_u = \frac{\partial f}{\partial u}, f_v = \frac{\partial f}{\partial v}$

If f is periodic in the first variable with wave number k, then for an integer q we denote by $f^{[q]}$ the q'th harmonic of f in its Fourier series. Explicitly:

$$f^{[q]}(v) = \frac{k}{2\pi}\int_0^{\frac{2\pi}{k}} du f(v) e^{-ikqu}$$

We also denote by $\langle f \rangle$ the average over x_1 of f:

$$\langle f \rangle = f^{[0]}$$

3 The Setting

Throughout this report, we consider a thin elastic sheet with a stretched edge. The sheet has thickness h, and the elastic material has Young's modulus E and Poisson ratio ν. Before any deformation occurs, the sheet covers a half-plane that is parametrized by $(u, v) \in \mathbb{R} \times [0, \infty)$ and embedded in $\mathbb{R}^3$ by the natural inclusion $(u, v) \mapsto (u, v, 0)$. In this configuration, the sheet's metric is the standard Euclidean metric in $\mathbb{R}^3$.

Next, we assume that the sheet is deformed along its edge parallel to the u-axis in such a way that the deformation is greatest nearest the edge, and is negligible far from it. This is expressed mathematically by saying that the elastic sheet has been endowed with a natural metric given by the tensor $\begin{pmatrix} (1+g(v))^2 & 0 \\ 0 & 1 \end{pmatrix}$, with g (the target metric) depending only on v and monotonically decreasing to 0 at infinity.

If $g \neq 0$ then the flat configuration of the sheet is unstable due to stress, and this stress is relieved by buckling. The buckling can be described via the displacement functions $X(u, v), Y(u, v)$ and $Z(u, v)$, such that the new parametrization of the sheet is

$$(u, v) \mapsto (u + X, v + Y, Z)$$

4 Bending Energy and Stretching Energy

Deviation of the sheet's configuration from the target metric increases the sheet's stretching energy, while local bending increases the bending energy. The sum of the stretching energy and the bending energy is the sheet's elastic energy. It can be shown by purely geometric considerations that the stretching energy is linear in h (the thickness of the sheet), whereas the bending energy is linear in h^3. For this reason configurations minimizing the metric deviation are preferred in thin sheets.

Before deformation, the flat configuration has zero elastic energy. Deforming the sheet has the effect that the flat configuration no longer matches the target metric and so has non-zero elastic energy. Hence, the flat configuration is in general not optimal, and the sheet buckles to compensate. The problem is thus to find the configuration given by X, Y and Z, having minimal energy. For this to be done, an energy functional assigning each configuration its elastic energy must be developed. The next few paragraphs follow the approach presented in [2].

In the small slope and small in-plane displacement approximations, the

strains of the surface are:

$$\epsilon_{uu} = X_u + \frac{Z_u^2}{2} - g(v)$$

$$\epsilon_{vv} = Y_v + \frac{Z_v^2}{2}$$

$$\epsilon_{uv} = \frac{Y_u + X_v + Z_u Z_v}{2}$$

This approximation is a generalization of the approximation upon which the FvK equations are built.

If $g(v)$ is small, the strains remain small, and based on Hookean elasticity A&B calculate the following energies:

Stretching energy:

$$\mathcal{E}_S = \int_0^\infty \int dudv \frac{Eh}{2(1-\nu^2)} \left[\nu(\epsilon_{uu} + \epsilon_{vv})^2 + (1-\nu)(\epsilon_{uu}^2 + 2\epsilon_{uv}^2 + \epsilon_{vv}^2)\right]$$

Bending energy:

$$\mathcal{E}_B = \int_0^\infty \int dudv \frac{Eh^3}{24(1-\nu^2)} (\Delta Z)^2$$

The total elastic energy is the sum of the stretching and bending energies:

$$\mathcal{E} = \mathcal{E}_S + \mathcal{E}_B$$

oNote that the maximum is independant of the Young's modulus E, and depends only on the target metric g and the Poisson ratio ν.

The integration domain along the u-axis hasn't been specified. Integrating over the entire domain of the variable u (all of $\mathbb{R}$) will, in general, lead to infinite energy. Hence the analysis is restricted to periodic solutions, meaning the integrations is done over a finite segment of the domain, and energy per unit length is considered rather than energy. The details of this are presented in the next section.

5 Restriction to Periodic Solutions

The analysis is restricted to periodic solutions in the u-axis. The solutions have wave numbers k, which will be determined by energy minimization. Since we are dealing exclusively with periodic solutions, the quantity that interests us for energy minimization is the elastic energy per period divided by the wavelength - the energy per unit length. Explicitly, this is:

$$\bar{\mathcal{E}_S} = \frac{k}{2\pi} \frac{Eh}{2(1-\nu^2)} \int_0^\infty \int_0^{\frac{2\pi}{k}} dudv \left(\left[\nu(\epsilon_{uu} + \epsilon_{vv})^2 + (1-\nu)(\epsilon_{uu}^2 + 2\epsilon_{uv}^2 + \epsilon_{vv}^2)\right]\right)$$

$$\bar{\mathcal{E}}_B = \frac{k}{2\pi} \frac{Eh^3}{24(1-\nu^2)} \int_0^\infty \int_0^{\frac{2\pi}{k}} dudv \left((\Delta Z)^2\right)$$

$$\bar{\mathcal{E}} = \bar{\mathcal{E}_S} + \bar{\mathcal{E}_B} \tag{5.1}$$

6 Audoly and Boudaoud's Approximation

The next step in a purely analytical treatment would be to give the equilibrium equations obtained by variation with respect to X, Y and Z (together with the boundary conditions imposed by periodicity). However, these have no analytical solutions in general and even their numerical solution is difficult [2], so from here on we proceed with the goal of minimizing the energy functional numerically.

The form of the energy functional in 5.1 is rather cumbersome, and a more compact expression is possible if we describe the functions as Fourier series. This form also lends itself quite naturally to the investigation of self-similarity.

Making use of the Parseval identity, and noting that the integrand in the stretching energy is made up entirely of quadratics in ϵ_{ij}, we have:

$$\bar{\mathcal{E}_S} = \frac{Eh}{2(1-\nu^2)} \int_0^\infty dv \sum_{q,q',i,i',j,j'} \epsilon_{ij}^{[q]} A_{ij,i'j'}^{q,q'} \epsilon_{i'j'}^{[q']}$$

where the coefficients $A_{ij,i'j'}^{q,q'}$ are determined by equation 5.1. For the bending energy we obtain the form:

$$\bar{\mathcal{E}_B} = \frac{Eh^3}{24(1-\nu^2)} \int_0^\infty dv \sum_{q=-\infty}^{\infty} \left| (\Delta Z)^{[q]} \right|^2$$

In order to ease the numerical minimization of the energy functional, A&B introduce the following approximation: For $q \neq 0$, they set $\epsilon_{uu}^{[q]} = 0$ and $\epsilon_{uv}^{[q]} = 0$. As is shown in appendix A, this yields X and Y in terms of Z, so that only one unknown function remains. This leads to the following energy functional, dependent only on $Z(u,v)$[1]:

$$\bar{\mathcal{E}} = \frac{Eh}{2(1-\nu^2)} \int_0^\infty dv \left[\left(\left\langle \frac{Z_u^2}{2} \right\rangle - g(v) \right)^2 + 2 \sum_{q>0} \left| \frac{\left\{ Z_{uu} Z_{vv} - Z_{uv}^2 \right\}^{[q]}}{k^2 q^2} \right|^2 + \frac{h^2}{12} \left\langle (\Delta Z)^2 \right\rangle \right] \tag{6.1}$$

7 Results

Having built the theoretical background, the next stage of the project was an attempt to numerically minimize 6.1. The technical details of minimization are provided in Appendix B. I tried to answer the following questions:

- Do the configurations found exhibit self-similarity?
- Are the configurations embeddings of the target metric?

[1] In [2] the functional differs in that the prefactor to the second term is $\frac{1}{2}$ rather than 2. However, inspection of the computer code used by A&B for their research reveals that the prefactor of 2 was in fact the one used for all calculations.

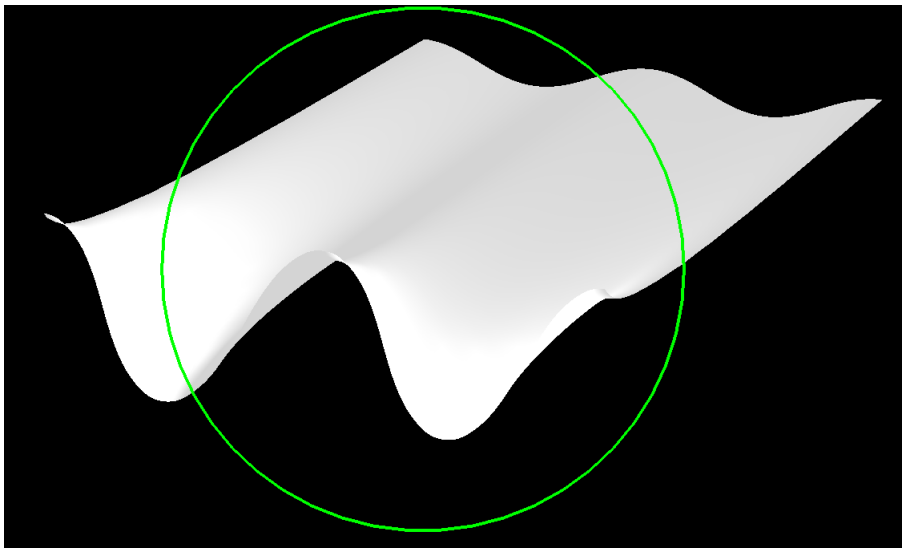

Fig. 7.1: A visualization of the surface resulting from minimizing the energy functional with respect to the target metric $g = \frac{1}{1+v}$ and $h = 10^{-5}$. Two periods of the resulting configuration are shown. There is no discernible self-similarity.

I investigated solutions resulting from the target metric $g(v) = \frac{1}{1+v}$, with different values for h.[2]

I ran simulations on a wide range of values for h and several different initial configurations. The results presented here reflect the lowest energy found for each thickness, even when they were obtained from different starting configurations.

As expected, for large values of h the configurations were generally close to the flat configuration, which minimizes the contribution of the bending energy. As h was lowered, the configurations became less harmonic, but closer to embeddings, hence lowering the contribution of the stretching energy.

My first goal was to ascertain whether the configurations found exhibit self-similarity. A visualization of a typical configuration for small h is shown in figure 7.1. There is no discernible self-similarity. In order to detect self-similarity analytically, [2] apply the following transform to Z, which they hypothesize would leave self-similar solutions invariant:

$$Z^{[3q]}(v) = \frac{1}{3} Z^{[q]}(3v) \sqrt{\frac{g(v)}{g(3v)}}$$

[2] Note that in [2] the family of metrics $g_\ell(v) = \frac{1}{1+v/\ell}$ is explored, with varying ℓ. As is shown in Appendix C, this is equivalent to leaving ℓ constant and varying h, as I've done.

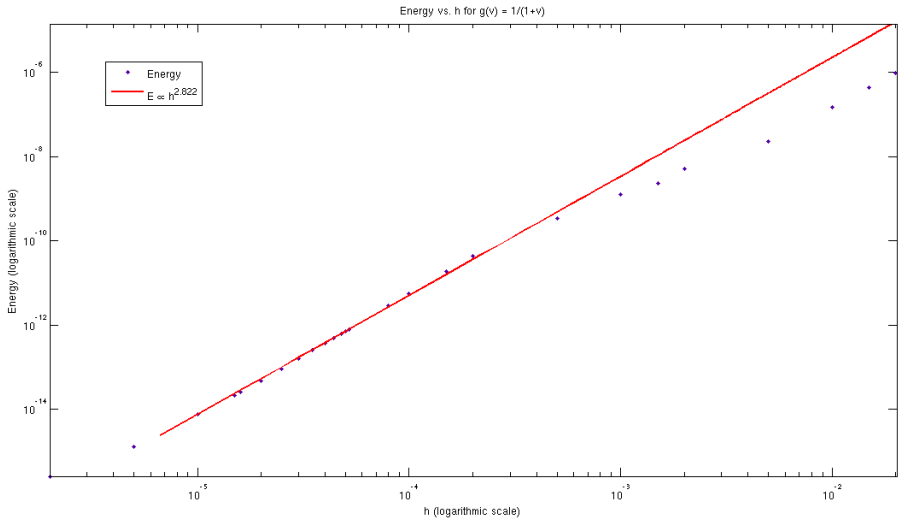

Fig. 7.2: The energy scaling as h approaches 0 for $g(v) = \frac{1}{1+v}$. The line is the best power law fit, giving $\bar{\mathcal{E}} \propto h^{2.379}$.

However, applying this transform to the configurations found did not leave them invariant. Since there is neither analytical evidence nor visual evidence of self-similarity, I had to conclude that the solutions found aren't self-similar.

It is still interesting to determine whether the configurations are embeddings, or near-embeddings, of the target metric in $\mathbb{R}^3$.

To this end, note that if for small enough h a metric embedding is the preferred configuration, it follows that the contribution of the stretching energy is zero and so the total elastic energy will approach zero at a rate of h^3 (the prefactor of the bending energy).

Indeed, the stretching energy decreases dramatically as h is lowered, indicating that the configurations approach (and perhaps converge to) embeddings in the limit $h \to 0$. However, the energy scaling doesn't approach 0 at a rate near h^3. Figure 7.2 shows the scaling of the energy as h approaches 0. The best power law fit is $\bar{\mathcal{E}} \propto h^{2.822}$. This is significantly lower than h^3, indicating that the configurations are not perfect embeddings.

7.1 Comparison with Results Obtained from Audoly and Boudaoud's Software

Basile Audoly kindly provided me with the software he used for the original calculations detailed in [2]. This enabled me to directly compare my own results with his. I compared the results with regard to the two points mentioned above, namely, whether the configurations found exhibited self-similarity, and whether

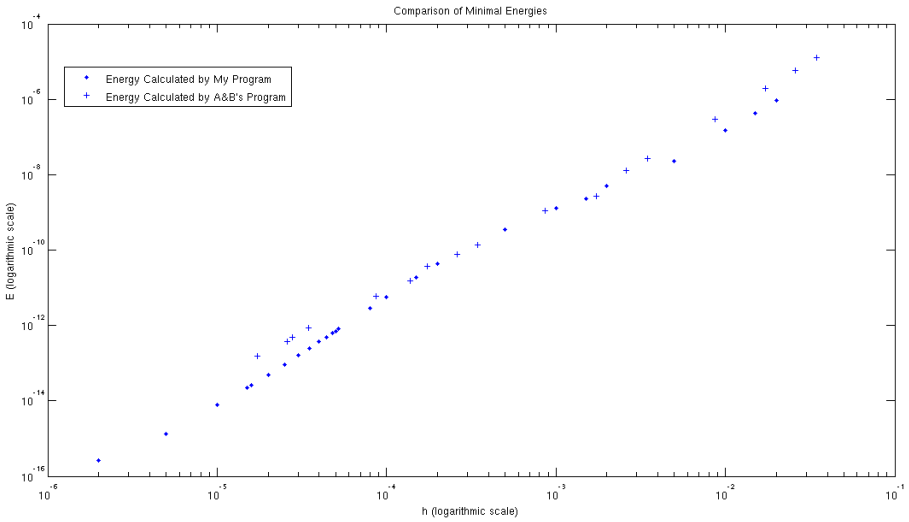

Fig. 7.3: Comparison of minimal energies calculated by my program and those calculated by A&B's program. The target metric is $g(v) = \frac{1}{1+v}$. It can be seen that the energies derived from A&B's program are higher than my own, with the difference most noticeable when h is small.

they were embeddings.

One of the features of Audoly's program is that it allows one to choose with respect to which frequencies the minimization is to be performed. The lowest energies were found when only frequencies of the form 3^p were allowed to change. This indeed resulted in self-similar configurations (very similar to the illustration in [2]). Interestingly, however, the energies themselves weren't lower than those of non-self-similar configurations found by my own program. Figure 7.3 shows values calculated by my program compared with those calculated by A&B's program. It can be seen that the values calculated by my program are somewhat lower than those calculated by A&B's program. In accordance, the energy scaling matching A&B's energies is about $h^{2.18}$ - significantly lower than my own.

The proper interpretation of the discrepancy between my own results and A&B's is unclear. The calculation involved - minimizing the energy functional of elastic sheets - is very difficult, and numerical simulations are extremely sensitive to a whole number of factors such as starting conditions and the specific algorithms used for the minimization. Beyond these fundamental limitations, there is also the possibility that I misused A&B's software, or made any number of other errors. Hence, the data represented in figure 7.3 shouldn't be interpreted as unequivocal evidence of the preference for non-self-similar configurations. Rather, it should serve as a warning that numerical results regarding

this problem should be taken with a grain of salt, at least before a fuller theoretical understanding is achieved.

A Derivation of the Simplified Energy Functional Based on A&B's Approximation

The A&B approximation is to set, for all $q \neq 0$, $\epsilon_{uu}^{[q]} = \epsilon_{uv}^{[q]} = 0$. In this appendix it's shown how this enables us to express X and Y in terms of Z only, and how this leads to the simplified form of the energy functional presented in equation 6.1.

We'll start with X: Recall that $\epsilon_{uu} = X_u + \frac{Z_u^2}{2} - g(v)$. Hence for all q $\epsilon_{uu}^{[q]} = X_u^{[q]} + \frac{(Z_u^2)^{[q]}}{2} - g^{[q]}(v)$. Since g depends only on v, for all $q \neq 0$ $g^{[q]} = 0$. So based on the A&B approximation, we have for all $q \neq 0$:

$$\epsilon_{uu}^{[q]} = 0 = X_u^{[q]} + \frac{\left(Z_u^2\right)^{[q]}}{2} = ikqX^{[q]} + \frac{\left(Z_u^2\right)^{[q]}}{2}$$

Rearranging, we have for all $q \neq 0$:

$$X^{[q]} = -\frac{1}{2ikq}\left(Z_u^2\right)^{[q]} \tag{A.1}$$

Applying similar manipulations to $\epsilon_{uv}^{[q]}$ (again, for $q \neq 0$):

$$2\epsilon_{uv}^{[q]} = 0 = Y_u^{[q]} + X_v^{[q]} + (Z_u Z_v)^{[q]} = ikqY^{[q]} + \left(X^{[q]}\right)_v + (Z_u Z_v)^{[q]} \tag{A.2}$$

Based on equation A.1:

$$\left(X^{[q]}\right)_v = -\frac{1}{ikq}\left(Z_u Z_{uv}\right)^{[q]}$$

Plugging this into equation A.2 and rearranging:

$$Y^{[q]} = -\frac{1}{k^2q^2}(Z_u Z_{uv})^{[q]} - \frac{(Z_u Z_v)^{[q]}}{ikq}$$

And by further manipulation:

$$Y^{[q]} = \frac{(Z_{uu} Z_v)^{[q]}}{k^2q^2} \tag{A.3}$$

We can now express all harmonics of X and Y besides the base harmonic in terms of Z. The base harmonics are chosen in such a way as to minimize the stretching energy, as follows: After rearranging the parts of equation 5.1 corresponding to the stretching energy and applying Parseval's formula we have:

$$\bar{\mathcal{E}_S} = \frac{Eh}{2(1-\nu^2)}\int_0^\infty dv\left[\left\langle\epsilon_{uu}^2\right\rangle + \left\langle\epsilon_{vv}^2\right\rangle + 2\nu\left\langle\epsilon_{uu}\epsilon_{vv}\right\rangle + 2(1-\nu)\left\langle\epsilon_{uv}^2\right\rangle\right]$$

By applying A&B's approximation:

$$\left\langle\epsilon_{uv}^2\right\rangle = \left\langle\epsilon_{uv}\right\rangle^2 = \left(\frac{\langle Y_u\rangle + \langle X_v\rangle + \langle Z_u Z_v\rangle}{2}\right)^2 = \left(\frac{\langle X_v\rangle + \langle Z_u Z_v\rangle}{2}\right)^2$$

By setting

$$X_v^{[0]} = -\langle Z_u Z_v \rangle \tag{A.4}$$

we can nullify the contribution of this component to the energy. Similarly, $\langle \epsilon_{vv}^2 \rangle = \sum_{q=-\infty}^{\infty} \left|\epsilon_{vv}^{[q]}\right|^2 = \left(\langle Y_v \rangle + \left\langle \frac{Z_v^2}{2} \right\rangle\right)^2 + 2\sum_{q>0} \left|\epsilon_{vv}^{[q]}\right|^2$, so we can reduce the contribution of this term by setting

$$Y_v^{[0]} = -\frac{1}{2}\left\langle Z_v^2 \right\rangle \tag{A.5}$$

Together, equations A.1, A.3,A.4 and A.5 (with the boundary condition $\lim_{v\to\infty} X^{[0]}(v) = \lim_{v\to\infty} Y^{[0]}(v) = 0$) give us a complete description of X and Y in terms of Z only. They also allow us to express $\bar{\mathcal{E}}$ in terms of Z only. The bending energy was, from the start, dependent only on Z, so we need not modify its form. As for the stretching energy, after the actions above we are left with:

$$\bar{\mathcal{E}_S} = \frac{Eh}{2(1-\nu^2)} \int_0^\infty dv \left[\left\langle \epsilon_{uu}^2 \right\rangle + \sum_{q\neq 0} \left|\epsilon_{vv}^{[q]}\right|^2 + 2\nu \left\langle \epsilon_{uu}\epsilon_{vv} \right\rangle \right]$$

However, because of the A&B approximation, $\epsilon_{uu}^{[q]} = 0$ for $q \neq 0$ on the one hand, and on the other $\epsilon_{vv}^{[0]} = 0$ based on the manipulations above. Hence $\langle \epsilon_{uu}\epsilon_{vv} \rangle = 0$. Additionally, because of the approximation, $\left\langle \epsilon_{uu}^2 \right\rangle = \langle \epsilon_{uu} \rangle^2$. So we're finally left with:

$$\bar{\mathcal{E}_S} = \frac{Eh}{2(1-\nu^2)} \int_0^\infty dv \left[\left(\left\langle \frac{Z_u^2}{2} \right\rangle - g(v) \right)^2 + 2\sum_{q>0} \left|\epsilon_{vv}^{[q]}\right|^2 \right] \tag{A.6}$$

Now, for q>0, using equation A.3:

$$\epsilon_{vv}^{[q]} = Y_v^{[q]} + \frac{1}{2}(Z_v^2)^{[q]} = \frac{(Z_{uuv}Z_v + Z_{uu}Z_{vv})^{[q]} - i^2k^2q^2\frac{1}{2}(Z_v^2)^{[q]}}{k^2q^2} = \frac{(Z_{uuv}Z_v + Z_{uu}Z_{vv})^{[q]} - ikq(Z_vZ_{uv})^{[q]}}{k^2q^2}$$

$$= \frac{(Z_{uuv}Z_v + Z_{uu}Z_{vv})^{[q]} - (Z_{uv}^2 + Z_vZ_{uuv})^{[q]}}{k^2q^2} = \frac{\left(Z_{uu}Z_{vv} - Z_{uv}^2\right)^{[q]}}{k^2q^2}$$

Hence:

$$2\sum_{q>0} \left|\epsilon_{vv}^{[q]}\right|^2 = 2\sum_{q>0} \left| \frac{\left\{Z_{uu}Z_{vv} - Z_{uv}^2\right\}^{[q]}}{k^2q^2} \right|^2$$

Plugging this into A.6, we have:

$$\bar{\mathcal{E}_S} = \frac{Eh}{2(1-\nu^2)} \int_0^\infty dv \left[\left(\left\langle \frac{Z_u^2}{2} \right\rangle - g(v) \right)^2 + 2\sum_{q>0} \left| \frac{\left\{Z_{uu}Z_{vv} - Z_{uv}^2\right\}^{[q]}}{k^2q^2} \right|^2 \right] \tag{A.7}$$

By adding this to the bending energy we have the energy functional presented in 6.1:

$$\bar{\mathcal{E}} = \frac{Eh}{2(1-\nu^2)} \int_0^\infty dv \left[\left(\left\langle \frac{Z_u^2}{2} \right\rangle - g(v) \right)^2 + 2 \sum_{q>0} \left| \frac{\left\{ Z_{uu} Z_{vv} - Z_{uv}^2 \right\}^{[q]}}{k^2 q^2} \right|^2 + \frac{h^2}{12} \left\langle (\Delta Z)^2 \right\rangle \right]$$

B Discretization and Minimization

In this appendix I present the details of the discretization and minimization process.

B.1 Discretization

The continuous form of the energy functional after the A&B approximation, as in equation 6.1, is:

$$\bar{\mathcal{E}} = \frac{Eh}{2(1-\nu^2)} \int_0^\infty dv \left[\left(\left\langle \frac{Z_u^2}{2} \right\rangle - g(v) \right)^2 + 2 \sum_{q>0} \left| \frac{\left\{ Z_{uu} Z_{vv} - Z_{uv}^2 \right\}^{[q]}}{k^2 q^2} \right|^2 + \frac{h^2}{12} \left\langle (\Delta Z)^2 \right\rangle \right]$$

There is no need to compare calculations for materials of differing Young's modulus and Poisson ratio, so we can safely discard the prefactor of $\frac{E}{2(1-\nu^2)}$. Additionally, the prefactor of h can be ignored, since it can easily be restored afterwards and has no bearing on the minimization process.

This leaves the functional to be minimized:

$$\int_0^\infty dv \left[\left(\left\langle \frac{Z_u^2}{2} \right\rangle - g(v) \right)^2 + 2 \sum_{q>0} \left| \frac{\left\{ Z_{uu} Z_{vv} - Z_{uv}^2 \right\}^{[q]}}{k^2 q^2} \right|^2 + \frac{h^2}{12} \left\langle (\Delta Z)^2 \right\rangle \right] \tag{B.1}$$

B.1 depends on the parameter h and k, as well as the continuous functions $Z^{[q]}(v)$ and $g(v)$ which must be discretized.

The first step is to choose a finite integration domain. To this end some $V > 0$ is chosen that is large enough s.t. $g(V) \ll g(0)$, and the integration domain is limited to $[0, V]$.

Second, some $Q \in \mathbb{N}$ is chosen that will be the highest non-zero harmonic in the function Z, so that $Z = \sum_{q=-Q}^{Q} Z^{[q]} e^{kqiu}$.

Next, a finite sequence of points $0 = v_0 < v_1 < \ldots v_{N-1} < v_N = V$ is chosen where the integrand will be evaluated. The points $g(v_i)$ and $z_i^{[q]} = Z^{[q]}(v_i), i = 0, 1, \ldots, N, q = 0, 1, \ldots, Q$ are given. However, this is not enough to evaluate the integrand; it depends on $Z_v^{[q]}$ and $Z_{vv}^{[q]}$ as well, which must be approximated. To this end central, forward and backward difference formulae are used, but the fact that the v_i may not be evenly spaced is liable to decrease precision. To circumvent this difficulty, the following construct is introduced: Define the points $x_i = \frac{i}{N}, i = 0, 1, \ldots, N$. We then choose a strictly increasing twice differentiable function $\varphi : [0, 1] \to [0, V]$ s.t. $\varphi(x_i) = v_i$. Define the function

$\zeta^{[q]} = Z^{[q]} \circ \varphi$. $Z^{[q]}$ can now be written as: $Z^{[q]} = \zeta^{[q]} \circ \varphi^{-1}$. $Z^{[q]}$'s derivatives derivatives can be expressed as:

$$Z_v^{[q]}(v_i) = \zeta_x^{[q]}(x_i)\left(\varphi^{-1}\right)_v(v_i) = \frac{\zeta_x^{[q]}(x_i)}{\varphi_x(x_i)}$$

$$Z_{vv}^{[q]}(v_i) = \frac{1}{\varphi_x(x_i)}\left[\zeta_{xx}^{[q]}(x_i) - \frac{\zeta_x^{[q]}(x_i)\varphi_{xx}(x_i)}{\varphi_x^2(x_i)}\right]$$

Since $Z^{[q]}$'s derivatives are expressed as depending on the derivatives of $\zeta^{[q]}$ and $\varphi^{[q]}$ only, and since both these functions are defined on evenly spaced grids central difference formulae can be used to evaluate them and gain a more precise approximation of $Z_v^{[q]}$ and $Z_{vv}^{[q]}$. Note that $Z_u^{[q]} = ikqZ^{[q]}$ and $Z_{uu}^{[q]} = -k^2q^2Z^{[q]}$, so we need make no special effort to obtain the derivatives by u.

In practice, I used central/forward/backward difference formulae with second-order precision. In addition, I limited my choice of the function φ to second-degree polynomials, which has the effect that the approximations of φ_x and φ_{xx} match exactly the analytical derivatives.

The integrand can now be evaluated at the points v_i. Once this is done, the energy can be calculated by integration using the trapezoidal rule.

B.2 Minimization

Once I developed a discrete form of the energy functional, I turned to the task of finding the optimal configuration of the sheet.

The variables are the complex coefficients $z_i^{[q]}$, with q ranging from 0 to Q and i ranging from 0 to N, as well as the wave number k. Hence the problem is to minimize a function from $\mathbb{R}^{2(N+1)(Q+1)+1}$ to $\mathbb{R}$. I used the implementation of the Broyden-Fletcher-Goldfarb-Shanno (BFGS) algorithm available in the Gnu Scientific Library (GSL). This method requires providing the function to be minimized as well as its derivatives with respect to each of the variables. Once the energy functional is expressed in its discrete form, calculating the derivatives was a straightforward, though technical, matter. The BFGS method requires an initial "guess", and proceeds to successively lower the evaluation of the function by using the information contained in the gradient and an estimation of the Hessian matrix. This continues until the norm of the gradient is deemed "small enough" by some measure provided by the user.

B.2.1 Choosing the Initial Configuration

It is clear from equation B.1 that the flat configuration ($z_i^{[q]} = 0$ for all i and q) is in (unstable) equilibrium, hence the gradient at this point is zero, and this cannot be the initial guess. Therefore, some thought must be given to the choice of the initial configuration.

First, from considerations of symmetry it can be seen that if only odd harmonics are excited, the even harmonics will remain zero throughout the minimization process. Similarly, if the excitement of all harmonics is done with

the same phase (for example by exciting only the real part), the same phase will remain throughout the minimization process. Hence, in order to allow the minimizer to make full use of all the variables at its disposal, the initial configuration must excite both odd and even harmonics, and contain some values that are out of phase with others. Additionally, I added the requirement that the initial configuration be "reasonable" in the sense that the deviation from the flat configuration should be greatest nearest the edge, and negligible near V.

In practice, experimentation showed that the minimization process is highly dependent on the starting configuration: whether the process eventually converges, the CPU usage, the final energy and the final configuration can each vary widely. The above were all also highly dependent on h (the non-variable thickness of the sheet). Surprisingly, the best results (i.e. with lowest energy) were achieved when the initial configuration involved exciting only of the real part of odd harmonics, which by the symmetries mentioned above meant the minimizer was limited at all stages to the real part of odd harmonics. This is contrary to the notion that allowing the minimizer more freedom in changing the configurations would yield lower energies. The high dependence of the outcome on initial conditions meant that the minimizations were all performed several times with different starting conditions. Generally, the best outcomes were achieved when the starting conditions for thicker sheets were, in fact, the final configurations of thinner sheets.

C Rescaling the Problem

There are a number of transformations that can be performed on the problem's parameters that result in essentially equivalent problems. I'll describe only one - rescaling along the v axis. This symmetry shows that varying the thickness of a sheet h, while leaving the rest of the system's features unchanged, is equivalent to varying the scaling of the target metric in the direction of the v-axis.

C.1 Rescaling Along the v Axis

Consider the problem given by $g'(v) = g(\alpha v)$ with $\alpha > 0$. Given displacement functions X,Y and Z and thickness h for the original problem, define the displacement functions $X'(u,v) = \alpha^{-1}X(\alpha u, \alpha v), Y'(u,v) = \alpha^{-1}Y(\alpha u, \alpha v), Z'(u,v) = \alpha^{-1}Z(\alpha u, \alpha v)$ for all v, and the new thickness $h' = \alpha^{-1}h$. Then:

$$\epsilon'_{uu}(u,v) = X_u(\alpha u, \alpha v) + \frac{1}{2}Z_u^2(\alpha u, \alpha v) - g(\alpha v) = \epsilon_{uu}(\alpha u, \alpha v)$$

And similarly:

$$\epsilon'_{uv}(u,v) = \epsilon_{uv}(\alpha u, \alpha v)$$
$$\epsilon'_{vv}(u,v) = \epsilon_{vv}(\alpha u, \alpha v)$$
$$\left(\Delta Z'(u,v)\right)^2 = \alpha^2 \left(\Delta Z(\alpha u, \alpha v)\right)^2$$

Applying this change of variables to equation 5.1, we see that the energy in the rescaled problem is $\alpha^{-2}\mathcal{E}$.

Here the problem has been rescaled based on the full functional; this rescaling will also give an equivalent problem once the functional is simplified with the A&B approximation.

References

[1] E. Sharon, B. Roman, M. Marder, G. S. Shin and H. L. Swinney, *Buckling Cascades in Free Sheets* Nature **419** 579 (2002).

[2] B. Audoly and A. Boudaoud, *Self-Similar Structures near Boundaries in Strained Systems* Physical Review Letters **91** 086105 (2003).